

Molecular fusion of fullerenes

A. Glotov¹, O. Knosp², R. Schmidt², and E.E.B. Campbell^{1,a}¹ Department of Experimental Physics, Göteborg University and Chalmers University of Technology, SE-41296 Göteborg, Sweden² Institut für Theoretische Physik, Technische Universität Dresden, D-01069 Dresden, Germany

Received 2 October 2000

Abstract. New experimental data is reported for the absolute cross sections for the fusion reaction channel in single gas-phase collisions between fullerenes. The experimental data is compared with the results of quantum mechanical and classical molecular dynamics simulations as well as with simple models. Quantum molecular dynamics simulations are in very good quantitative agreement with the experimental data. The overall dynamical behaviour can be well-described qualitatively in the framework of simple models.

PACS. 36.40.-c Atomic and molecular clusters

1 Introduction

Fullerenes are interesting model systems for studying the dynamics of systems with a large but finite number of degrees of freedom [1]. In our laboratory we have been studying fullerene-fullerene collisions in the intermediate collision energy regime (50-5000 eV) where a number of competing reaction channels occur: scattering [2], fusion [3–5], evaporation, (multi-)fragmentation [4] and charge transfer [2,6]. The fusion reaction channel is particularly interesting since there are many similarities but also some important differences compared to the dynamics of nuclear collisions [7]. Our early experiments considered only the reaction products within a small scattering angle range about 0° [7,6]. The more recent work has concentrated on the scattering angle dependence of the fragmentation [4] and charge transfer [2] products and is able to provide considerable insight into the collision dynamics as well as to confirm the earlier interpretations in terms of simple models. These results indicated that the earlier work had underestimated the magnitude of the fusion cross sections because of scattering of the product out of the detection window due to multiple unimolecular dissociation reactions on a timescale of up to microseconds after the collision. In the present paper we present new measurements of the absolute cross sections for molecular fusion, taking the scattering of products into consideration. The values obtained for the cross sections are significantly larger than the original reports for collision energies higher than 100 eV. The collisions are also studied theoretically by employing the molecular dynamics (MD) strategy, both from quantum mechanical [8] and classical [9] approaches. We show that the quantum molecular dynamics approach, in contrast to classical molecular dy-

namics, provides a very good quantitative description of the collision energy dependence of the reaction.

2 Experimental setup

The experimental apparatus has been described in detail before [3,4] and will be described only briefly here. A positively charged fullerene ion beam is produced in the source vacuum chamber by evaporating fullerene powder from an oven at a temperature of about 500 °C and ionising by electron impact. The ions are extracted into the main scattering vacuum chamber by a pulsed electric field. Collision energies of interest for the fusion reaction lie in the range 60-500 eV (centre of mass). The ions with desired mass-to-charge ratio are mass-selected and directed into the scattering cell. The scattering cell is a cylindrical oven with a circular entrance of 2 mm diameter and a horizontal exit slit of 2 mm height allowing the detection of scattered ions at laboratory angles up to 80°. Fullerene powder of high purity (commercially available, ≥ 99.4% C₆₀ or C₇₀) is evaporated inside the cell forming the target gas. The positively charged products of the collision reaction are detected by a time-of-flight reflectron mass spectrometer. The reflectron can be rotated around the scattering cell in the horizontal plane allowing the determination of the angular distribution of ions. The kinetic energy of the detected ions can be determined by applying a positive potential on a grid in the front of the detector. The energy spread of the parent ion beam was measured to be 5% (FWHM) of the laboratory collision energy, and the angular spread was measured to be (2±0.5)° (FWHM) which determined the angular resolution for the range of interest in the present experiments.

^a e-mail: f3aec@fy.chalmers.se

3 Theoretical approach

The classical MD model used in the present work employs the empirical Brenner-I potential [10] and was described in Ref. [9] where it was used to calculate trajectories for fullerene–noble-gas-atom collisions. The quantum mechanical MD model is a hybrid of the density functional methodology together with empirical potentials and has also been described in detail before [11]. Both MD models were used in this work to calculate collision trajectories for a total collision time up to several pico-seconds after impact. For each collision energy, trajectories for different initial relative orientations of the fullerene cages were explored.

4 Results and discussion

The fusion channel in fullerene-ion–fullerene-neutral collisions (FFC) has been studied as a function of collision energy and scattering angle. In spite of the rather high collision energies, the full product (C_{120}^* , C_{130}^* , C_{140}^*) of the completely inelastic collision can survive for collision energies just above the fusion threshold, on the μs time-scale of the experiment and be detected. A weakly van-der-Waals-bound dimer could not survive under these conditions. Instead, many bonds are broken and re-formed to again produce a fullerene-like compound. As the collision energy is increased further the fusion product undergoes increasing numbers of unimolecular dissociation steps. The observed fragmentation behavior close to threshold (multiple C_2 evaporation) supports our conclusion that the fusion product has a re-formed fullerene-like structure. A number of different MD studies [8, 12, 13] have shown that the most probable compound has a “peanut-like” geometrical structure. Such a peanut-like structure has a binding energy approximately twice that of the two individual fullerenes. This is a local minimum on the potential energy surface and on a long enough time-scale should relax to a more strongly bound isomer such as the “cigar” or the more compact “sphere” [14] if fragmentation does not happen before the rearrangement can take place.

Fig. 1 shows the cross section for the $C_{60}^+ + C_{60} \rightarrow C_{120}^{+*} \rightarrow C_n^+ + \sum a_i C_{m_i}$ reaction (where $\sum a_i m_i = (120 - n)$). The new experimental data (open triangles) lie significantly higher than our earlier reported results (filled squares) and a finite, although very small, fusion signal can be detected for collision energies as high as 400 eV (*ca.* 0.02 \AA^2 but with rather large error bars due to the low signals and complexity of the data analysis). Our recent measurements were able to show that the abrupt drop at just below 200 eV seen in the early measurements was due mainly to a change in fragmentation behaviour (from C_2 evaporation to the break-up of the cage into larger chain and ring fragments), leading to increased scattering, [4], as had been suggested to explain the original measurements [7]. The data have been compared to two simple phenomenological models in Fig. 1. These models have been discussed in detail previously [3, 7]. A simple absorbing sphere model (ASM) predicts a linear dependence of

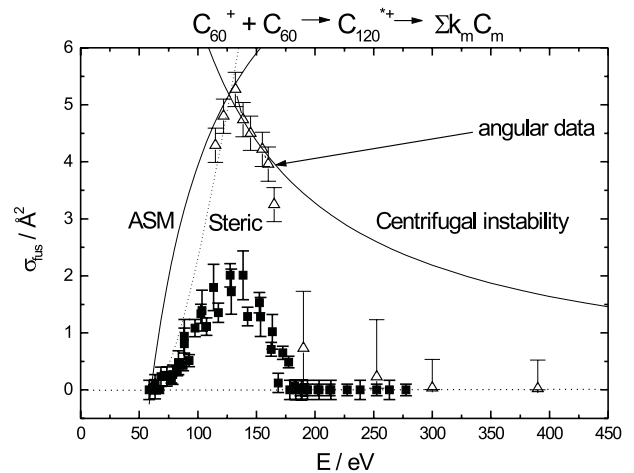


Fig. 1. Fusion cross section as a function of the collision energy for $C_{60}^+ + C_{60}$ collisions. Squares: earlier data [3]. Triangles: present data. Full line: behaviour expected from simple ASM. Dotted line: behaviour expected with steric correction to ASM.

the cross section as $(1 - E_{th}/E)$ close to the energetic threshold E_{th} . If the angular momentum in the collision exceeds a certain critical value ℓ_{cr} then the fused compound is unstable and cannot survive the collision due to the centrifugal forces. Beyond the critical energy E_{cr} , given by:

$$E_{cr} = E_{th} + \frac{\hbar^2 \ell_{cr}^2}{2\mu R^2}$$

where R is the sum of the radii of the collision partners, the cross section is predicted to fall linearly as $1/E$. A much better fit to the data at energies below the critical value is obtained by invoking a steric effect in the ASM. The observed fusion cross section is much lower than the geometrical cross section. The ASM fit assumes a constant average “fusion probability” on the order of a few percent. The steric model (SM) assumes that the fusion probability increases with increasing collision energy. This is a simple way of accounting for the dependence of the fusion probability on the relative orientation of the cages [5]. The SM fit, which predicts an increase of the cross section proportional to $(E - E_{th})^2/E$, allowed us to obtain a reliable value for the energetic threshold for fusion [3]. Since there is no significant loss due to scattering for collision energies below *ca.* 100 eV, the experimentally-derived values for the energetic threshold for fusion after the new experiments and data analysis are unchanged. The new experimental results are in better agreement with the collision energy dependence predicted by the simple steric model. The very abrupt drop in cross section reported previously is no longer quite so apparent. A good comparison with the model at high collision energies, where the cross section is predicted to fall due to centrifugal instability, and where strong fragmentation of the fusion product occurs is very difficult due to the large error bars in the experimental values. However, the experimental cross sections still seem to drop somewhat faster than the simple model predicts.

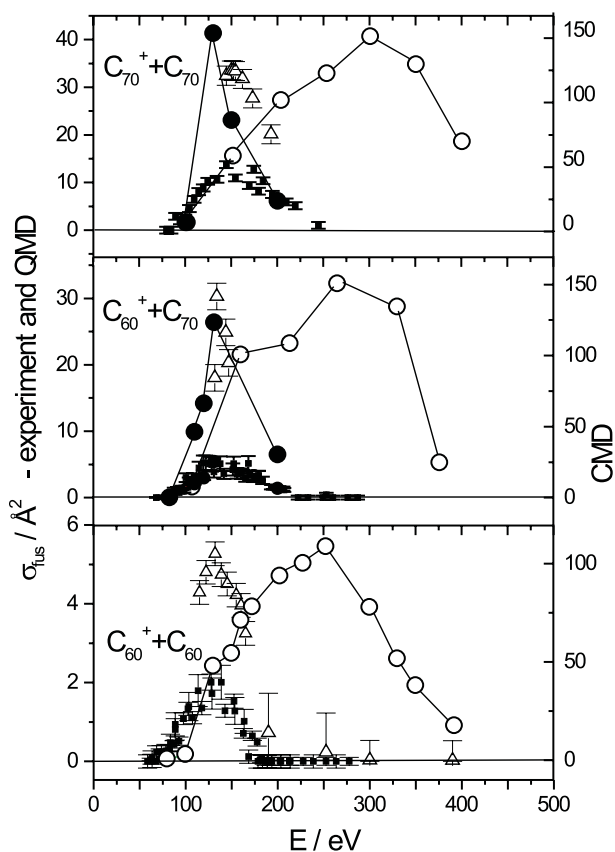


Fig. 2. Fusion cross sections as a function of collision energy for three different collision pairs. Squares: earlier data [3]. Triangles: present data. Left y -axis shows experimental and QMD scale (filled circles), right y -axis shows CMD scale (open circles).

As was discussed earlier [1], both quantum [8] and classical [15,16] molecular dynamics calculations are able to reproduce the experimentally determined energetic barrier for fusion as long as the initial internal energy of the fullerene projectile ion is taken into consideration. However, if the absolute value of the cross section and the energy window for the fusion reaction are considered then only the quantum molecular dynamics calculations are able to provide good agreement with the data. Comparisons are shown in Fig. 2 for all three collision systems.

With the increase of the total number of carbon atoms in the colliding partners the maximum of the fusion cross section increases, together with the value of the fusion barrier and the width of the fusion window. This can be partly understood in terms of the increasing geometrical cross section in the collisions, the increased stability of C_{70} , compared to C_{60} and the increase in the number of vibrational degrees of freedom as the size of the collision partners is increased leading to a greater overall stability. The geometrical cross sections for the three collision systems are 154, 166 and 179 \AA^2 , respectively. Therefore, the values for the measured absolute fusion cross sections, compared to the geometrical cross sections, are still very small, even after correcting for the effect of scattering. The

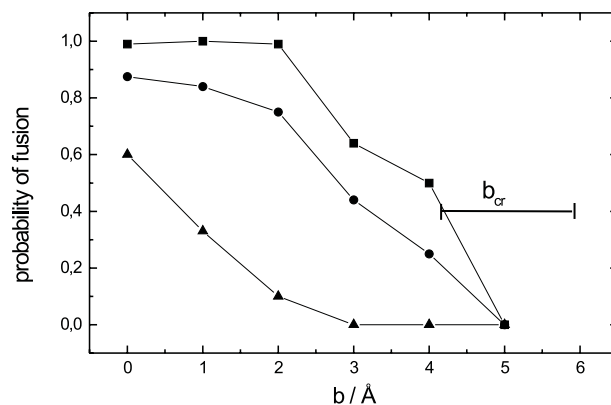


Fig. 3. Calculated fusion probability for $C_{70}^+ + C_{70}$ collisions using QMD. Each point averages over 8-10 trajectories with different initial orientations. The range of experimentally determined b_{cr} for the equivalent collision energies is shown for comparison. Up triangles: 120 eV; squares: 150 eV; circles: 160 eV.

absolute value of the cross section as well as the width of the fusion window are very well reproduced by the quantum molecular dynamics simulations (full dots in Fig. 2). Each point in the QMD calculations was obtained by averaging over 48-60 trajectories. The colliding fullerenes were given a temperature of 2000 K prior to collision to match the experimental conditions. Fusion was defined in the calculations as having occurred when a product larger than the projectile and target masses was present at the end of a trajectory calculation (2 ps). This method is likely to underestimate the theoretical fusion cross section at high collision energies > 250 eV [4]) where all fragments are small non-fullerene-like rings and chains, however, it should be reliable for the plotted data that all lie below this collision energy. The agreement with the experimental data is extremely good. The reason for the extremely low absolute values for fusion is the strong tendency, pointed out previously [5], for the fullerenes to bounce away from each other even if the collision energy exceeds the fusion barrier and the impact parameter lies below the critical value. The probability for fusion depends on the initial relative orientation of the fullerene cages. As the collision energy increases the number of initial orientations that can lead to fusion also increases. This is illustrated in Fig. 3 for $C_{70}^+ + C_{70}$ collisions.

The probability for obtaining a C_{140} 2 ps after the collision is plotted as a function of the impact parameter in Fig. 3 for three different collision energies. In these calculations the initial temperature of the fullerenes was 0 K. (As was discussed previously [8] for the value of the fusion threshold, zero temperature collisions are equivalent to finite temperature collisions where the total internal energy is the same. *I.e.* the collision energies in Fig. 3 can be compared to experimental collision energies that are 25 eV lower, where 25 eV is the total internal energy before collision.) Each point in Fig. 3 has been obtained from averaging over 8-10 trajectories with different initial orientations. As the collision energy increases more of these

initial orientations can produce fusion. This leads to the large difference in the results for 120 eV and 150 eV. This is the origin of the steric correction to the absorbing sphere model, discussed above. However, as the collision energy is increased the centrifugal energy also increases leading to a greater instability of the fused compound and therefore an overall reduction in the probability. The range of the experimentally determined critical impact parameters b_{cr} beyond which the system is unstable due to centrifugal forces has also been indicated on the figure for the relevant energies. This is also seen to be in very nice agreement with the calculations.

The CMD model does not provide good quantitative agreement with the experiments. It can reproduce the fusion threshold but vastly overestimates the magnitude of the fusion cross section. The maxima predicted by the CMD model lie close to the geometrical values and the energetic window in which fusion products can be detected is predicted to be much larger than that observed experimentally (note the different y -axis scale for the CMD results in Fig. 2).

In summary, the fusion reaction between two colliding fullerenes can be qualitatively well described in the framework of a simple phenomenological model. The absolute cross section values are significantly lower than the geometrical values due to the tendency of the fullerenes to bounce apart, depending on the initial relative orientation of the two cages. The absolute cross section values are well reproduced quantitatively using QMD calculations. CMD can reproduce the energetic threshold for fusion but greatly overestimates the absolute value of the cross section and the width of the fusion window.

Financial support from the Swedish Natural Sciences Research Council (NFR) is gratefully acknowledged.

References

1. E.E.B. Campbell, F. Rohmund, Rep. Prog. Phys. **63**, 1061 (2000).
2. A.V. Glotov, E.E.B. Campbell, Chem. Phys. Lett. **327**, 61 (2000).
3. F. Rohmund, A. Glotov, K. Hansen, E.E.B. Campbell, J. Phys. B. **29**, 5143 (1996).
4. A.V. Glotov, E.E.B. Campbell, Phys. Rev. A **62**, 033202 (2000).
5. F. Rohmund, E.E.B. Campbell, O. Knospe, G. Seifert, R. Schmidt, Phys. Rev. Lett. **76**, 3289 (1996).
6. F. Rohmund, E.E.B. Campbell, J. Phys. B **30**, 5293 (1997).
7. E.E.B. Campbell, F. Rohmund, A.V. Glotov, Nuovo Cimento A **110**, 1191 (1997).
8. O. Knospe, A.V. Glotov, G. Seifert, R. Schmidt, J. Phys. B **29**, 5163 (1996).
9. R. Ehlich, E.E.B. Campbell, O. Knospe, R. Schmidt, Z. Phys. D **28**, 153 (1993).
10. D.W. Brenner, Phys. Rev. B **42**, 9458 (1990); corrections in Phys. Rev. B **46**, 1948 (1990).
11. G. Seifert, R. Schmidt, New J. Chem. **16**, 1145 (1992); O. Knospe, R. Schmidt, G. Seifert, Adv. Class. Traject. Meth. **4**, 153 (1999).
12. D. Tomanek, M.A. Schluter, Phys. Rev. Lett. **67**, 2331 (1991).
13. Y. Xia, Y. Mu, C. Tan, Y. Xing, H. Yang, Nucl. Inst. Meth. Phys. Res. B **129**, 356 (1997).
14. D.L. Strout, R.L. Murry, C. Xu, W.C. Eckhoff, G.K. Odom, G. Scuseria, Chem. Phys. Lett. **214**, 576 (1993).
15. D.H. Robertson, D.W. Brenner, C.T. White, J. Phys. Chem. **99**, 15721 (1995).
16. B.L. Zhang, C.Z. Wang, C.T. Chan, K.M. Ho, J. Phys. Chem. **97**, 3134 (1993).